scientific reports

Check for updates

OPEN

Effect of texture and color enhancement imaging on the visibility of gastric tumors

Hiroaki Sakai[1,3], Naoto Iwai[1,2,3]✉, Osamu Dohi[2], Kohei Oka[1,2], Takashi Okuda[1,2], Toshifumi Tsuji[1], Kengo Okabe[1,2], Tomoya Ohara[1,2], Mariko Kajiwara-Kubtota[1], Hayato Fukui[1], Junichi Sakagami[1], Keizo Kagawa[1], Ken Inoue[2], Naohisa Yoshida[2], Kazuhiko Uchiyama[2], Tomohisa Takagi[2], Hideyuki Konishi[2] & Yoshito Itoh[2]

Texture and color enhancement imaging (TXI) may improve the visibility of gastric tumors and allow their early detection. However, few reports have examined the utility of TXI. Between June 2021 and October 2022, 56 gastric tumors in 51 patients undergoing endoscopic submucosal dissection at Fukuchiyama City Hospital were evaluated preoperatively using conventional white light imaging (WLI), narrow-band imaging (NBI), and TXI modes 1 and 2. The color differences of the tumors and surrounding mucosae were evaluated using the CIE 1976 L*a*b color space, Additionally, the visibility scores were scaled. Of the 56 gastric tumors, 45 were early gastric cancers, and 11 were adenomas. Overall, the color difference in TXI mode 1 was considerably higher compared to WLI (16.36 ± 7.05 vs. 10.84 ± 4.05; $p < 0.01$). Moreover, the color difference in early gastric cancers was considerably higher in TXI mode 1 compared to WLI, whereas no significant difference was found in adenomas. The visibility score in TXI mode 1 was the highest, and it was significantly higher compared to WLI. Regarding adenomas, the visibility score in TXI mode 1 was also significantly higher compared to that in WLI. TXI may provide improved gastric tumor visibility.

Keywords Adenoma, Early gastric cancer, Texture and color enhancement imaging, Visibility, White light imaging

Gastric cancer is the fifth leading cause of cancer mortality in the world[1]. Early detection of gastric tumors using esophagogastroduodenoscopy (EGD) allows early endoscopic treatment. However, 4.6–54.3% of gastric tumors may be missed by this diagnostic method[2–6]. Conventional white light imaging (WLI) has been widely employed for screening the stomach; however, image enhanced endoscopy (IEE) is anticipated to provide the improved detection[7].

Texture and color enhancement imaging (TXI), which was introduced in 2020 (Olympus Corporation, Tokyo, Japan)[8], optimizes the visualization of three elements: structure, color tone, and brightness. First, the input image of WLI is split into a texture image and a base image. Next, texture enhancement and brightness adjustment are performed for each image. Thereafter, the images are re-combined and output as TXI mode 2. Then, color enhancement is conducted to output as TXI mode 1. TXI enhances subtle changes in the color tone and structure of the images that are difficult to recognize with WLI. Therefore, TXI may improve the visibility of gastric tumors and allow early detection of such malignancies; however, only a few such studies have been conducted[9–15]. Therefore, we aimed to investigate the visibility of gastric tumors by use of TXI.

Methods

Study design

During this retrospective study, we evaluated 71 gastric tumors in 66 patients undergoing endoscopic submucosal dissection (ESD) for gastric tumors at Fukuchiyama City Hospital between June 2021 and October 2022. Of the 71 tumors, 14 lacked endoscopic images and one was diagnosed as a neuroendocrine tumor during the pathological examination; therefore, they were excluded from the study. Finally, 56 tumors in 52 patients were included

[1]Department of Gastroenterology and Hepatology, Fukuchiyama City Hospital, Fukuchiyama, Kyoto, Japan. [2]Molecular Gastroenterology and Hepatology, Graduate School of Medical Science, Kyoto Prefectural University of Medicine, 465 Kawaramachi Hirokoji Kamigyo-ku, Kyoto 602-8566, Japan. [3]These authors contributed equally: Hiroaki Sakai and Naoto Iwai. ✉email: na-iwai@koto.kpu-m.ac.jp

(Fig. 1). This study was conducted in accordance with the ethical principles of the Declaration of Helsinki, and its protocol was approved by the Institutional Review Board (IRB) of Fukuchiyama City Hospital (approval number 4–38). For this study, informed consent has been waived by the IRB of Fukuchiyama City Hospital due to the anonymity and retrospective nature of the study, and patients were given the option to be excluded from the study using the opt-out approach.

Collecting endoscopic images and ESD

To obtain images of the tumors and perform the ESD procedures, nine operators used the EVIS X1 endoscopic system with a GIF-H290Z endoscope (Olympus Medical Systems Corporation, Tokyo, Japan) until March 2022; however, beginning in April 2022, the GIF-EZ1500 endoscope was used. Endoscopic images were obtained using WLI, narrow-band imaging (NBI), and TXI modes 1 and 2 by each endoscopists prior to ESD. ESD was carried out according to Japanese guidelines[16]. The resected specimens were histopathologically assessed by the clinical pathologists.

Color difference analysis

The color difference between the tumor and the surrounding mucosa was assessed as an objective index. A straight line was drawn on the tumor image, and two points were plotted for each tumor and the surrounding mucosa on the line. Figure 2 presents the representative images of one of the tumors, with four plotted areas (17×17 pixels) on the line. The colors of the plotted areas were quantified using Affinity Photo version 1.10.4 (Serif, Inc., Nottingham, UK). Quantification was performed using the CIE 1976 L*a*b color space[17], with L* axis representing brightness, the a* axis representing red-to-green chromaticity, and the b* axis representing yellow-to-blue chromaticity. The color values of the areas inside the tumors minus their surrounding mucosae were represented as ΔL*, Δa*, and Δb*, respectively. The color difference (ΔE) was evaluated using the following equation:

$$\Delta E = \left[(\Delta L*)^2 + (\Delta a*)^2 + (\Delta b*)^2\right]^{1/2}$$

The average of the two-color differences on was calculated for each tumor and compared among WLI, NBI, and TXI modes 1 and 2. Then, the ΔL*, Δa*, and Δb* values of WLI and TXI mode 1 were compared.

Visibility score analysis

The visibility scores were scaled as a subjective index. The nine operators, consisting of 3 experts (≥ 100 cases of ESD) and 6 trainees (< 100 cases of ESD), evaluated the visibility of each gastric tumor after ESD[18]. The visibility scores of NBI and TXI modes 1 and 2 were compared with those of WLI according to the following scale: + 2 (remarkably improved), + 1 (improved), 0 (unchanged), − 1 (worsened), and − 2 (remarkably worsened). Figure 3 presents one of the tumors and its visibility scores.

Statistical analysis

Quantitative variables are expressed as the mean ± standard deviation. Comparisons were carried out using the Wilcoxon signed-rank test. Statistical significance was defined as $p < 0.05$. All statistical analyses were carried out using JMP version 15.2.1 (SAS Institute Inc., Cary, NC, USA).

Results

Table 1 describes the clinicopathologic characteristics of the patients, lesions, and types of scopes used. The mean age was 72.8 years, and 36 patients were male among the 52 patients. Forty-five lesions were early gastric cancer, and 11 were adenomas. Among the 45 early gastric cancers, 40 were intestinal type, and 5 were diffuse type. *Helicobacter pylori* infection of 42 lesions (75%) were eradicated. The GIF-H290Z endoscope was used for 40 lesions, and the GIF-EZ1500 endoscope was used for 16 lesions.

Table 2 describes the color differences in each mode. Overall, the color differences in TXI mode 1 and 2 were considerably higher than that in WLI. Moreover, the color difference in TXI mode 1 was considerably higher than

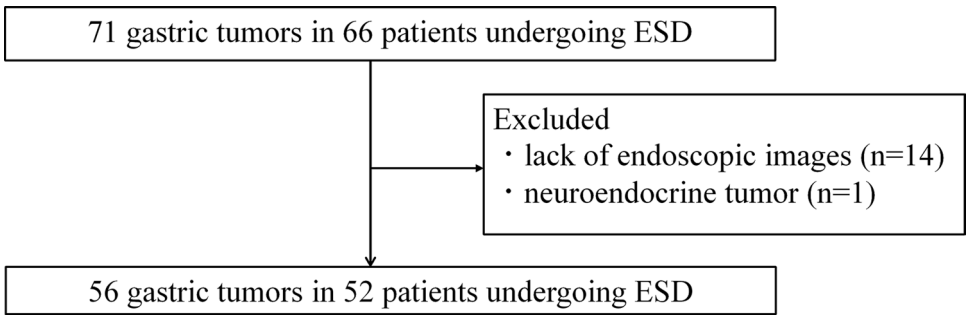

Figure 1. Study flowchart. ESD, endoscopic submucosal dissection.

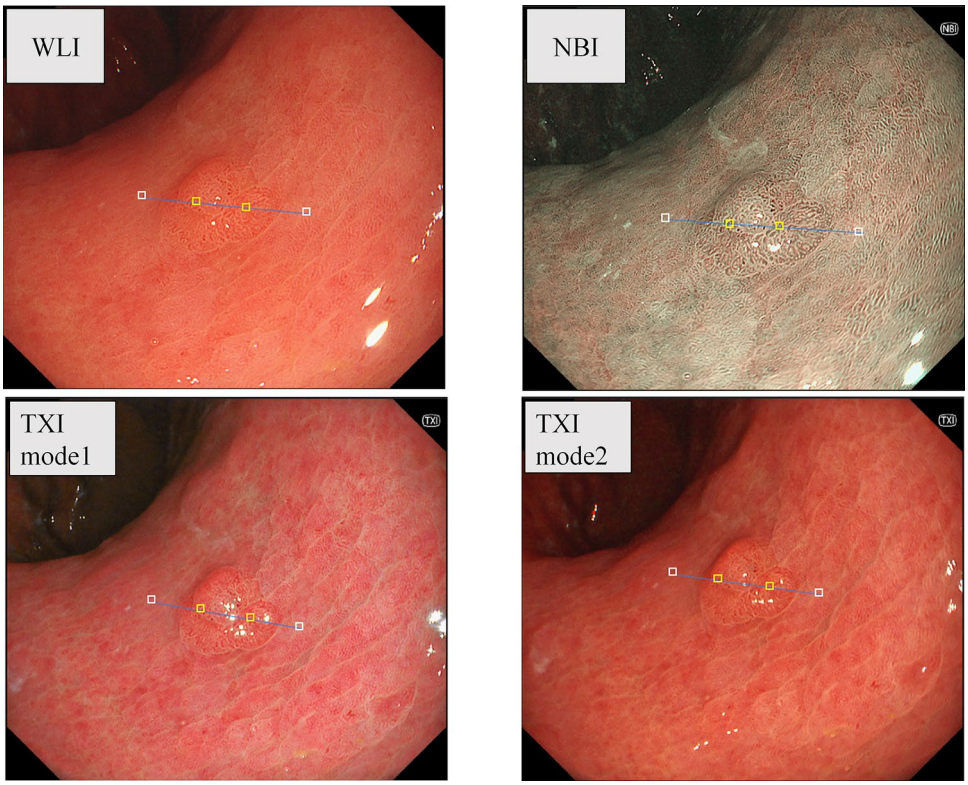

Figure 2. Representative images of gastric tumors before endoscopic submucosal dissection (ESD) obtained using white light imaging (WLI), narrow-band imaging (NBI), and texture and color enhancement imaging (TXI) modes 1 and 2. A straight line was drawn on the tumor image, and two areas (17 × 17 pixels) were plotted for each tumor and its surrounding mucosa on the line to calculate the color difference.

that in WLI (16.36 ± 7.05 vs. 10.84 ± 4.05; $p < 0.01$), NBI (16.36 ± 7.05 vs. 12.92 ± 6.33; $p < 0.01$), and TXI mode 2 (16.36 ± 7.05 vs. 13.11 ± 5.41; $p < 0.01$). A subgroup analysis revealed that the color difference of early gastric cancers was significantly higher in TXI mode 1 than in WLI (17.29 ± 7.17 vs. 10.82 ± 3.92; $p < 0.01$), whereas adenomas exhibited no significant difference (12.59 ± 5.03 vs. 10.94 ± 4.56; $p = 0.64$). The color difference in TXI mode 1 was higher than that in WLI, regardless of *H. pylori* infection status, tumor size, coloration, morphological type, or type of scope used during the procedure.

The ΔL*, Δa*, and Δb* values of the gastric tumors and surrounding mucosae observed with WLI and TXI mode 1 are shown in Table 3. Overall, the Δa* and Δb* values achieved with TXI mode 1 were considerably higher than those achieved with WLI. However, the ΔL* value achieved with TXI mode 1 was significantly lower than that achieved with WLI. For early gastric cancers, the Δa* and Δb* values achieved with TXI mode 1 were considerably higher than those achieved with WLI. Additionally, the ΔL* value achieved with TXI mode 1 was lower than that achieved with WLI. However, the difference was not significant. For adenomas, the Δ*a and Δb* values achieved with TXI mode 1 and WLI were not significantly different; however, the ΔL* value achieved with TXI mode 1 was significantly lower than that achieved with WLI.

The visibility scores of the gastric tumors are presented in Table 4. The mean visibility score was significantly higher in TXI mode 1 compare to WLI (0.95 ± 0.67; $p < 0.01$) and TXI mode 2 (0.95 ± 0.67 vs. 0.54 ± 0.60; $p < 0.01$), whereas no difference was found between TXI mode1 and NBI (0.95 ± 0.67 vs. 0.80 ± 0.83; $p = 0.47$). The visibility scores were significantly higher in TXI mode 1 compared to WLI during all subgroup analyses. Regarding adenomas, the visibility scores in TXI mode 1 were significantly higher compared to WLI, whereas those in NBI and TXI mode 2 were not.

Discussion

In this retrospective study, which included 56 gastric tumors, we examined the color differences and the visibility scores. The color differences and visibility scores of TXI modes 1 and 2 were significantly higher than those of WLI. Furthermore, the color differences and visibility scores of TXI mode 1 were significantly higher than those of TXI mode 2. We revealed that TXI, especially TXI mode 1, could improve the visibility of gastric tumors compared to WLI during objective and subjective evaluations.

IEE technology such as NBI[19], blue laser imaging-bright[20], and linked color imaging[21], has been used to provide the improved detection of gastric lesions. TXI, which is another new IEE technology, is available in clinical settings. However, it remains largely unknown how we should use TXI mode when we perform esophagogastroduodenoscopy through early gastric cancer screening. Furthermore, it remains unclear how to use different

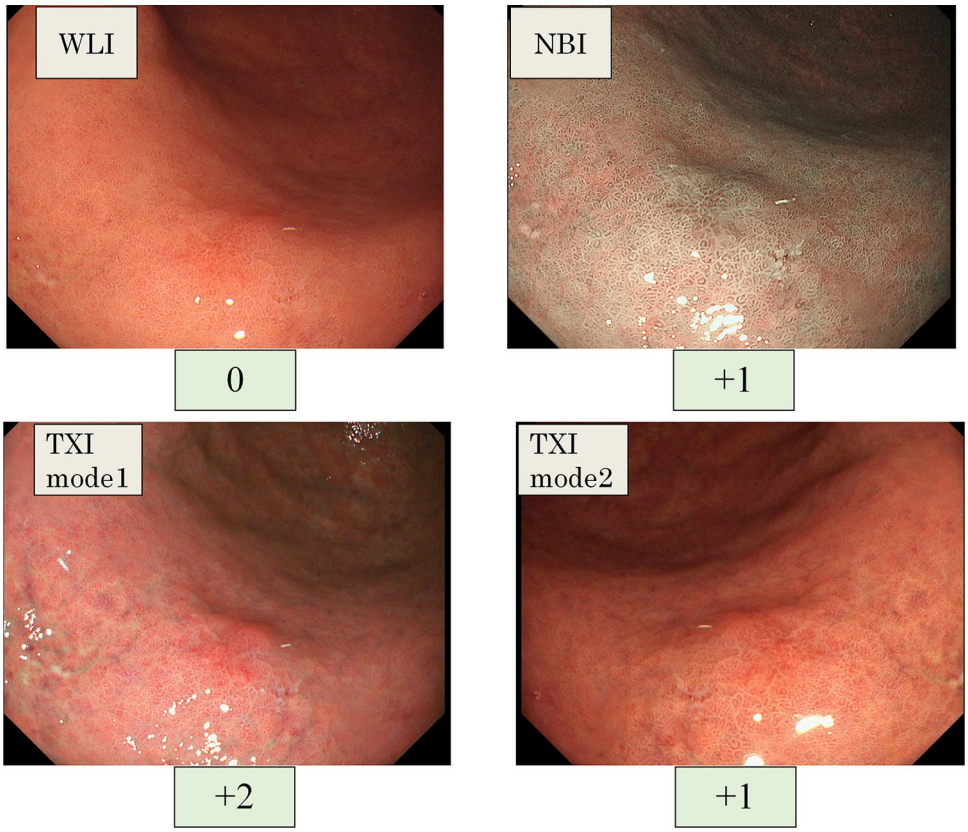

Figure 3. Representative images of gastric tumors and visibility scores. The visibility scores of narrow-band imaging (NBI) and texture and color enhancement imaging (TXI) modes 1 and 2 were compared with those white light imaging (WLI). The visibility scores were as follows: + 2 (remarkably improved), + 1 (improved), 0 (unchanged), − 1 (worsened), and − 2 (remarkably worsened).

Patient characteristics	(n = 52)
Age, mean ± SD (years)	72.8 ± 8.8
Sex, male/female (n)	36/16
Lesion characteristics	(n = 56)
Histological diagnosis, early gastric cancer/adenoma (n)	45/11
Histological type, intestinal type/diffuse type (n)	40/5
H. pylori infection status, positive/eradicated/negative (n)	12/42/2
Tumor size, ≥ 10/ < 10 mm (n)	23/33
Color, reddish/discolored (n)	33/23
Morphological type, 0-I/IIa/IIb/IIc/complex/SMT-like (n)	3/26/8/11/6/2
Type of scope used during the procedure	(n = 56)
Scope, GIF-H290Z/GIF-EZ1500 (n)	40/16

Table 1. Clinicopathologic characteristics. SD, standard deviation; SMT, submucosal tumor.

IEEs, including TXI mode and NBI, for this screening. Thus, we aimed to assess the visibility of gastric tumors with respect to TXI mode.

We demonstrated that the color difference in TXI mode 1 was considerably higher compared to that in WLI, as reported by previous studies[9–11,13]. Some studies have reported that the color difference in TXI mode 2 was not significantly higher than that in WLI[9,10]. However, other studies have reported significant differences, similar to our study[12,13]. The discrepancy could be influenced by the number of enrolled cases, as the studies suggesting no differences had ≤ 20 cases. Additionally, we found that the use of TXI mode 1 resulted in higher visibility scores than those obtained with WLI, similar to previous reports[9,10,13,15]. Collectively, our study revealed that TXI mode 1 could provide advantages compared to WLI when used during objective and subjective evaluations.

		WLI	NBI	TXI mode 1	TXI mode 2
All (n = 56)	Mean ± SD	10.84 ± 4.05	12.92 ± 6.33	16.36 ± 7.05	13.11 ± 5.41
	p values (vs. WLI)		0.02	< 0.01	< 0.01
	p values (vs. NBI)			< 0.01	0.80
	p values (vs. TXI mode 2)			< 0.01	
Early gastric cancer (n = 45)	Mean ± SD	10.82 ± 3.92	12.98 ± 6.72	17.29 ± 7.17	13.68 ± 5.42
	p values (vs. WLI)		0.05	< 0.01	< 0.01
Adenoma (n = 11)	Mean ± SD	10.94 ± 4.56	12.69 ± 4.40	12.59 ± 5.03	10.80 ± 4.73
	p values (vs. WLI)		0.15	0.64	0.76
H. pylori infection: positive (n = 12)	Mean ± SD	11.46 ± 3.64	12.28 ± 4.69	19.20 ± 8.42	15.15 ± 4.65
	p values (vs. WLI)		0.68	< 0.01	< 0.01
H. pylori infection: eradicated (n = 42)	Mean ± SD	10.76 ± 4.22	13.13 ± 6.82	15.36 ± 6.43	12.27 ± 5.41
	p values (vs. WLI)		0.02	< 0.01	0.06
Tumor size ≥ 10 mm (n = 23)	Mean ± SD	11.91 ± 5.05	14.07 ± 6.84	17.57 ± 7.86	13.31 ± 5.25
	p values (vs. WLI)		0.05	< 0.01	0.03
Tumor size < 10 mm (n = 33)	Mean ± SD	10.10 ± 2.96	12.12 ± 5.81	15.52 ± 6.29	12.97 ± 5.52
	p values (vs. WLI)		0.18	< 0.01	< 0.01
Reddish color (n = 33)	Mean ± SD	10.68 ± 3.72	12.64 ± 5.60	16.42 ± 6.60	12.60 ± 4.42
	p values (vs. WLI)		0.07	< 0.01	< 0.01
Discolored (n = 23)	Mean ± SD	11.08 ± 4.47	13.33 ± 7.23	16.28 ± 7.65	13.84 ± 6.51
	p values (vs. WLI)		0.17	< 0.01	0.07
Morphological type IIa (n = 26)	Mean ± SD	11.63 ± 4.55	13.19 ± 7.90	17.40 ± 7.19	13.41 ± 5.17
	p values (vs. WLI)		0.43	< 0.01	0.04
Morphological types IIb and IIc (n = 19)	Mean ± SD	9.67 ± 3.06	12.80 ± 4.90	14.57 ± 6.40	12.41 ± 5.54
	p values (vs. WLI)		0.03	< 0.01	0.02
GIF-290Z (n = 40)	Mean ± SD	11.17 ± 3.92	12.34 ± 5.43	17.72 ± 7.34	14.06 ± 5.35
	p values (vs. WLI)		0.25	< 0.01	< 0.01
GIF-EZ1500 (n = 16)	Mean ± SD	10.03 ± 4.26	14.38 ± 7.97	12.98 ± 4.82	10.73 ± 4.78
	p values (vs. WLI)		0.02	0.01	0.74

Table 2. Color differences between the gastric tumors and surrounding mucosae. SD, standard deviation; WLI, white light imaging; NBI, narrow-band imaging; TXI, texture and color enhancement imaging.

			WLI	TXI mode 1
All (n = 56)	ΔL*	Mean ± SD	1.77 ± 6.86	0.68 ± 8.59
		p values (vs. WLI)		0.02
	Δa*	Mean ± SD	3.58 ± 5.94	6.62 ± 10.59
		p values (vs. WLI)		< 0.01
	Δb*	Mean ± SD	2.50 ± 2.84	3.75 ± 4.65
		p values (vs. WLI)		0.01
Early gastric cancer (n = 45)	ΔL*	Mean ± SD	0.66 ± 6.78	-0.04 ± 9.13
		p values (vs. WLI)		0.18
	Δa*	Mean ± SD	4.18 ± 5.90	7.69 ± 10.64
		p values (vs. WLI)		< 0.01
	Δb*	Mean ± SD	2.57 ± 2.99	4.21 ± 4.68
		p values (vs. WLI)		< 0.01
Adenoma (n = 11)	ΔL*	Mean ± SD	6.32 ± 5.10	3.64 ± 4.83
		p values (vs. WLI)		< 0.01
	Δa*	Mean ± SD	1.14 ± 5.44	2.23 ± 9.14
		p values (vs. WLI)		0.95
	Δb*	Mean ± SD	2.23 ± 2.09	1.86 ± 4.01
		p values (vs. WLI)		0.51

Table 3. ΔL*, Δa*and Δb* between gastric tumors and the surrounding mucosae. SD, standard deviation; WLI, white light imaging; TXI, texture and color enhancement imaging.

		NBI	TXI mode 1	TXI mode 2
All (n = 56)	Mean ± SD	0.80 ± 0.83	0.95 ± 0.67	0.54 ± 0.60
	p values (vs. WLI)	< 0.01	< 0.01	< 0.01
	p values (vs. NBI)		0.47	
	p values (vs. TXI mode 2)	0.04	< 0.01	
Early gastric cancer (n = 45)	Mean ± SD	0.84 ± 0.79	1.02 ± 0.65	0.62 ± 0.61
	p values (vs. WLI)	< 0.01	< 0.01	< 0.01
Adenoma (n = 11)	Mean ± SD	0.64 ± 0.98	0.64 ± 0.64	0.18 ± 0.39
	p values (vs. WLI)	0.11	0.03	0.5
Helicobacter pylori infection: positive (n = 12)	Mean ± SD	1.00 ± 0.82	1.08 ± 0.64	0.50 ± 0.50
	p values (vs. WLI)	0.01	< 0.01	0.03
H. pylori infection: eradicated (n = 42)	Mean ± SD	0.79 ± 0.83	0.93 ± 0.67	0.55 ± 0.62
	p values (vs. WLI)	< 0.01	< 0.01	< 0.01
Tumor size ≥ 10 mm (n = 23)	Mean ± SD	0.74 ± 0.79	0.83 ± 0.64	0.43 ± 0.50
	p values (vs. WLI)	< 0.01	< 0.01	< 0.01
Tumor size < 10 mm (n = 33)	Mean ± SD	0.85 ± 0.86	1.03 ± 0.67	0.61 ± 0.65
	p values (vs. WLI)	< 0.01	< 0.01	< 0.01
Reddish color (n = 33)	Mean ± SD	0.67 ± 0.80	0.97 ± 0.72	0.48 ± 0.56
	p values (vs. WLI)	< 0.01	< 0.01	< 0.01
Discolored (n = 23)	Mean ± SD	1.00 ± 0.83	0.91 ± 0.58	0.61 ± 0.64
	p values (vs. WLI)	< 0.01	< 0.01	< 0.01
Morphological type IIa (n = 26)	Mean ± SD	0.85 ± 0.95	0.96 ± 0.65	0.46 ± 0.57
	p values (vs. WLI)	< 0.01	< 0.01	< 0.01
Morphological types IIb and IIc (n = 19)	Mean ± SD	0.95 ± 0.69	1.11 ± 0.64	0.74 ± 0.64
	p values (vs. WLI)	< 0.01	< 0.01	< 0.01
GIF-290Z (n = 40)	Mean ± SD	0.83 ± 0.83	1.03 ± 0.65	0.63 ± 0.62
	p values (vs. WLI)	< 0.01	< 0.01	< 0.01
GIF-EZ1500 (n = 16)	Mean ± SD	0.75 ± 0.83	0.75 ± 0.66	0.31 ± 0.46
	p values (vs. WLI)	0.01	< 0.01	0.06

Table 4. Visibility scores of gastric tumors. SD, standard deviation; WLI, white light imaging; NBI, narrow-band imaging; TXI, texture and color enhancement imaging.

A comparison between TXI modes 1 and 2 revealed that TXI mode 1 was superior in both color difference and visibility score. This could be due to the fact that color enhancement is conducted in TXI mode 1, based on the images from TXI mode 2.

During subgroup analyses of early gastric cancers, the color difference in TXI mode 1 was higher than those in WLI. In contrast, for adenomas, the color difference was not different from that in WLI. During this study, the color difference was quantified according to the L*a*b* color space. On the L* axis which represents brightness, the ΔL* value was lower in TXI mode 1 than WLI, especially in adenomas. This may be because brightness in dark areas is more enhanced with TXI than with WLI[8]. Therefore, it is possible that the difference in brightness between the tumor and surrounding mucosa was smaller in TXI, especially in adenomas. In contrast, the Δa* and Δb* values were higher in TXI mode 1 than WLI, especially in early gastric cancers. These findings indicated that TXI mode 1 could offer higher color saturation between the tumor and surrounding mucosa, resulting in higher color differences for early gastric cancers.

Previous studies have addressed the usefulness of TXI for pharyngeal or esophageal lesions suggesting squamous cell carcinoma[22], duodenal tumors[23], and colorectal lesions[24–30]. Antonelli G et al. recently performed a randomized trial and demonstrated the utility of TXI for the detection of colorectal neoplasia[30]. For gastric lesions, Kadota et.al. have recently reported that third-generation NBI provided the higher detection rate of gastric neoplasms in comparison to WLI and TXI mode 1[31]. Our data revealed that the color difference in TXI mode 1 was significantly higher than that in NBI, while no differences were observed in the visibility scores between TXI mode 1 and NBI. The discrepancy between our results and their findings may possibly be influenced by insufficient experience of TXI mode 1.

This study has some limitations. First, this was a single-center, retrospective study. Because of its retrospective data and a limited number of cases, the presence of selection bias cannot be excluded. Thus, our findings need to be validated in a larger population. Second, the endoscopic images were not captured under the same conditions; therefore, the points plotted in the images that were obtained by each IEE were slightly different. Third, both the GIF-H290Z and GIF-EZ1500 endoscopes were used during this study. A previous study revealed that the visibility scores achieved with GIF-XZ1200 were higher than those achieved with GIF-H290Z[15]. Thus, our findings should be validated by using a variety of endoscopes. In summary, our findings suggest that TXI may provide the improved visibility of gastric tumors and allow the early detection of gastric tumors.

Data availability

The data in this study are available from the corresponding author on reasonable request.

Received: 1 July 2024; Accepted: 14 August 2024
Published online: 18 August 2024

References

1. Bray, F. *et al.* Global cancer statistics 2022: GLOBOCAN estimates of incidence and mortality worldwide for 36 cancers in 185 countries. *CA Cancer J. Clin.* **74**, 229–263 (2024).
2. Suvakovic, Z. *et al.* Improving the detection rate of early gastric cancer requires more than open access gastroscopy: a five year study. *Gut* **41**, 308–313 (1997).
3. Hosokawa, O. *et al.* Diagnosis of gastric cancer up to three years after negative upper gastrointestinal endoscopy. *Endoscopy* **30**, 669–674 (1998).
4. Voutilainen, M. E. & Juhola, M. T. Evaluation of the diagnostic accuracy of gastroscopy to detect gastric tumours: Clinicopathological features and prognosis of patients with gastric cancer missed on endoscopy. *Eur. J. Gastroenterol. Hepatol.* **17**, 1345–1349 (2005).
5. Vradelis, S., Maynard, N., Warren, B. F., Keshav, S. & Travis, S. P. Quality control in upper gastrointestinal endoscopy: Detection rates of gastric cancer in Oxford 2005–2008. *Postgrad. Med. J.* **87**, 335–339 (2011).
6. Oka, K. *et al.* Clinical features of false-negative early gastric cancers: A retrospective study of endoscopic submucosal dissection cases. *Gastroenterol. Res. Pract.* **2021**, 6635704. https://doi.org/10.1155/2021/6635704 (2021).
7. Yao, K. *et al.* Guidelines for endoscopic diagnosis of early gastric cancer. *Dig. Endosc.* **32**, 663–698 (2020).
8. Sato, T. TXI: Texture and color enhancement imaging for endoscopic image enhancement. *J. Healthc. Eng.* **2021**, 5518948. https://doi.org/10.1155/2021/5518948 (2021).
9. Ishikawa, T. *et al.* Efficacy of texture and color enhancement imaging in visualizing gastric mucosal atrophy and gastric neoplasms. *Sci. Rep.* **11**, 6910. https://doi.org/10.1038/s41598-021-86296-x (2021).
10. Abe, S. *et al.* Visibility of early gastric cancer in texture and color enhancement imaging. *DEN Open* **2**, e46. https://doi.org/10.1002/deo2.46 (2022).
11. Kawasaki, A. *et al.* Usefulness of third-generation narrow band imaging and texture and color enhancement imaging in improving visibility of superficial early gastric cancer: A study using color difference. *DEN Open* **3**, e186. https://doi.org/10.1002/deo2.186 (2023).
12. Koyama, Y. *et al.* Visibility of early gastric cancers by texture and color enhancement imaging using a high-definition ultrathin transnasal endoscope. *Sci. Rep.* **13**, 1994. https://doi.org/10.1038/s41598-023-29284-7 (2023).
13. Shijimaya, T. *et al.* Usefulness of texture and color enhancement imaging (TXI) in early gastric cancer found after Helicobacter pylori eradication. *Sci. Rep.* **13**, 6899. https://doi.org/10.1038/s41598-023-32871-3 (2023).
14. Kemmoto, Y. *et al.* Higher detectability of gastric cancer after *Helicobacter pylori* eradication in texture and color enhancement imaging mode 2 in screening endoscopy. *DEN Open* **4**, e279. https://doi.org/10.1002/deo2.279 (2024).
15. Futakuchi, T. *et al.* Texture and color enhancement imaging improves the visibility of gastric neoplasms: clinical trial with image catalogue assessment using conventional and newly developed endoscopes. *BMC Gastroenterol.* **23**, 389. https://doi.org/10.1186/s12876-023-03030-9 (2023).
16. Ono, H. *et al.* Guidelines for endoscopic submucosal dissection and endoscopic mucosal resection for early gastric cancer (second edition). *Dig. Endosc.* **33**, 4–20 (2021).
17. Kuehni, R. G. Color-tolerance data and the tentative CIE 1976 L a b formula. *J. Opt. Soc. Am.* **66**, 497–500 (1976).
18. Oka, K. *et al.* Red dichromatic imaging improves visibility of bleeding during gastric endoscopic submucosal dissection. *Sci. Rep.* **13**, 8560. https://doi.org/10.1038/s41598-023-35564-z (2023).
19. Yoshida, N. *et al.* Early gastric cancer detection in high-risk patients: A multicentre randomised controlled trial on the effect of second-generation narrow band imaging. *Gut* **70**, 67–75 (2021).
20. Dohi, O. *et al.* Blue laser imaging-bright improves the real-time detection rate of early gastric cancer: A randomized controlled study. *Gastrointest. Endosc.* **89**, 47–57 (2019).
21. Ono, S. *et al.* Linked color imaging focused on neoplasm detection in the upper gastrointestinal tract: A randomized trial. *Ann. Intern. Med.* **174**, 18–24 (2021).
22. Dobashi, A. *et al.* Texture and color enhancement imaging increases color changes and improves visibility for squamous cell carcinoma suspicious lesions in the pharynx and esophagus. *Diagnostics (Basel)* **11**, 2021. https://doi.org/10.3390/diagnostics11111971 (1971).
23. Okimoto, K. *et al.* Magnified endoscopy with texture and color enhanced imaging with indigo carmine for superficial nonampullary duodenal tumor: a pilot study. *Sci. Rep.* **12**, 10381. https://doi.org/10.1038/s41598-022-14476-4 (2022).
24. Nishizawa, T. *et al.* TXI (texture and color enhancement imaging) for serrated colorectal lesions. *J. Clin. Med.* **11**, 119. https://doi.org/10.3390/jcm11010119 (2021).
25. Yoshida, N. *et al.* Analysis of texture and color enhancement imaging for improving the visibility of non-polypoid colorectal lesions. *Dig. Dis. Sci.* **67**, 5657–5665 (2022).
26. Toyoshima, O. *et al.* Texture and color enhancement imaging in magnifying endoscopic evaluation of colorectal adenomas. *World J. Gastrointest. Endosc.* **14**, 96–105. https://doi.org/10.4253/wjge.v14.i2.96 (2022).
27. Tamai, N. *et al.* Visibility evaluation of colorectal lesion using texture and color enhancement imaging with video. *DEN Open* **2**, e90. https://doi.org/10.1002/deo2.90 (2022).
28. Sakamoto, T. *et al.* Detection of colorectal adenomas with texture and color enhancement imaging: Multicenter observational study. *Dig. Endosc.* **35**, 529–537 (2023).
29. Yoshida, N. *et al.* Additional 30-second observation of the right-sided colon for missed polyp detection with texture and color enhancement imaging compared with narrow band imaging: A randomized trial. *Am. J. Gastroenterol.* **119**, 539–546 (2024).
30. Antonelli, G. *et al.* Texture and color enhancement imaging versus high definition white-light endoscopy for detection of colorectal neoplasia: A randomized trial. *Endoscopy* **55**, 1072–1080 (2023).
31. Kadota, T. *et al.* Comparison of effective imaging modalities for detecting gastric neoplasms: A randomized three-arm phase II trial. *Am. J. Gastroenterol.* https://doi.org/10.14309/ajg.0000000000002871 (2024).

Acknowledgements

We thank Masashi Taniguchi, Chie Hattori, Tasuku Hara, Shinya Okishio, and Toshiyuki Komaki for data collection and insightful comments. We thank all members of Molecular Gastroenterology and Hepatology, Graduate School of Medical Science, Kyoto Prefectural University of Medicine.

Author contributions

Conception and design: H.S. and N.I.; Collection and assembly of data: H.S., N.I., K.O., T.O., T.T., K.O., T.O., M.K.-K., H.F., and J.S.; Data analysis and interpretation: H.S., N.I., and O.D.; Manuscript preparation: H.S. and N.I.; Revision of the manuscript: O.D., K.K., K.I., N.Y., K.U., T.T., H.K., and Y.I.; Final approval of manuscript: All authors.

Competing interests

The authors declare no competing interests.

Additional information

Correspondence and requests for materials should be addressed to N.I.

Reprints and permissions information is available at www.nature.com/reprints.

Publisher's note Springer Nature remains neutral with regard to jurisdictional claims in published maps and institutional affiliations.